Electronic Structure and Spectroscopic Properties of the Two Structural Isomers of Donor−Acceptor Substituted Sesquifulvalene in the Gas and Solution Phases—A Case Study of Sudden Polarization

Tapas Kar,[†] Nabamita Panja,[‡] and Prasanta Kumar Nandi*[,‡]

Department of Chemistry and Biochemistry, Utah State University, Logan, Utah 84322-0300, and Department of Chemistry, Bengal Engineering and Science University, Shibpur, Howrah 711 103, India

Received: June 27, 2006; In Final Form: September 13, 2006

The ground state equilibrium structure and electric properties of two structural isomers of donor−acceptor substituted sesquifulvalene have been calculated at ab initio HF and MP2 levels for different conformations. The electronic properties of low lying excited singlets are calculated by using CI calculations including single excitations only. Isomer **I** in which the inter-ring charge transfer (CT) is reinforced in the presence of substituents shows sudden polarization in the ground and two lower lying excited states, while isomer **II** in which the longitudinal CT interaction is attenuated does not exhibit sudden polarization. The phenomenon of sudden polarization has been rationalized in terms of the easy polarization, smaller rotational barrier, and enhanced inter-ring CT on going from the planar to the orthogonal geometry. The appreciably large static second-order polarizability of **I** stems from its sudden polarized ground state. The solvent (using the conductor-like polarizable continuum model (CPCM)) plays a significant role on the modulation of ground and excited state electronic properties which, in general, predicts blue-shifts for **I**. However, for molecule **II**, the two lower energy transitions show a red-shift while the others show a weaker blue-shift at any conformation.

1. Introduction

It has long been known that in ethylene and longer polyenes the rotation around the π-bond by 90° causes large polarization which in turn leads to appreciably large charge separation in some excited singlet states which are characterized by strong enhancement in the dipole moment and linear polarizability.[1−12] This phenomenon named as "sudden polarization" was first introduced by Salem.[3] The ionic character of the valence excited states arises from the easy polarizability of the alkenes as a result of small internal perturbation.[2] The sudden polarization of ethylene was discussed earlier[4−7] on the basis of one-sided pyramidalization, and later on,[8] one-sided scissoring deformation was found to be essential to explain its nonadiabatic photochemistry. The phenomenon of sudden polarization was also studied critically in connection with the rotation about a double bond in substituted polyenes, for example, retinal when optically excited.[9,10] The effect can be made pronounced in the presence of the electric field arising from the electronic asymmetry of the molecule or the electric field due to polar solvent, and so forth (external perturbation), in which case the charge transfer between the twisted moieties can be effectively augmented at 90°. Ramasesha and Albert[11,12] considered a number of conjugated polyenes with varying chain lengths and push−pull strengths to investigate sudden polarization in these species. In the Hückel model, they obtained[11] a sharp peak of linear polarizability (α) for polyene in both the ground and excited states at 90°. However, using the interacting Pariser−Parr−Pople (PPP) model Hamiltonian, the authors[12] showed that one or more of the low lying dipole allowed excited singlet states of push−pull substituted polyenes can exhibit sudden polarization which is rather independent of the actual positions of the substituents provided the electronic asymmetry is maintained.

Other kinds of molecules showing sudden polarization in the ground state have received overwhelming attention in the study of nonlinear optical (NLO) properties. The earlier theoretical study of the NLO responses of 4-quinopyran derivatives[13,14] showed rather strong enhancement of first hyperpolarizability (β) when the rings were twisted around 90°. This has been ascribed to the huge amount of charge transfer (CT) accompanying the transition, neutral quinoid → the charged benzenoid. Recently, Marks et al.[15] using high level theoretical calculations obtained the highest value of static β at nearly the perpendicular conformation for merocyanine-type chromophores. Sesquifulvalene hydrocarbon is another interesting molecular system which shows enhanced polarization and NLO responses[16,17] when the rings are twisted by 90°. However, the phenomenon of sudden polarization was studied most extensively on the substituted polyenes. We, therefore, intend to explore this aspect in the case of sesquifulvalene (a polar hydrocarbon) with proper modification of its electronic asymmetry by introducing donor−acceptor substituents. For this purpose, we have considered two isomers of the sesquifulvalene molecule (Scheme 1) which differ only in the position of the substituents. The electronic structure and charge transfer characteristics of the chosen molecules have been studied by employing a sufficiently high level of ab initio quantum mechanical methods. The conductor-like polarizable continuum model (CPCM)[18,19] has been used to find the solvent effect on the ground state structure and the spectroscopic properties of the molecules. The solvents considered in the present study include chloroform ($\epsilon = 4.9$), acetone ($\epsilon = 20.7$), and water ($\epsilon = 78.4$).

* Corresponding author. E-mail: nandi_pk@yahoo.co.in. Fax: +91 33 2668 2916.
[†] Utah State University.
[‡] Bengal Engineering and Science University.

10.1021/jp0640124 CCC: $33.50
Published on Web 10/20/2006

SCHEME 1

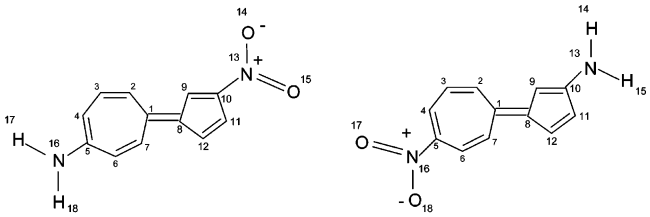

(I) **(II)**

2. Method of Calculations

2.1. Calculation of the Electronic Structure and Properties in the Gas Phase. The ground state geometry of molecules **I** and **II** at different inter-ring torsion angles (ϕ) has been fully optimized at the RHF/6-31+G** level. The effect of electron correlation (EC) on the planar and perpendicular ground state geometry is calculated at the MP2 level using the same basis set. The electric multipole moments of each molecule are calculated at the respective equilibrium geometry. Additionally, the single point MP2/6-31+G** calculations are performed at the HF geometry to obtain energy and one electron properties. The transition energy along with the spectroscopic parameters of a few low lying excited singlet states of the chosen isomers at different ϕ are calculated by the routinely used CIS calculation with the 6-31+G** basis set. In the CIS calculation, about 16 lowest energy molecular orbitals (MOs) out of 56 occupied MOs are kept frozen and the single excitations from the remaining occupied MOs to all the 296 unoccupied MOs have been considered. Therefore, the present CIS calculation is expected to provide sufficiently accurate results. For a given ϕ, the electronic energy (E) of an excited state has been calculated as $E = E_0$ (MP2/6-31+G**//HF/6-31+G** calculated ground state energy) + ΔE (transition energy obtained at the HF equilibrium geometry).

The energy of an uncharged molecule due to the first-order electrostatic interaction with a weak static electric field can be written as[20,21]

$$E \equiv E(F_i, F_{ij}, F_{ijk}, F_{ijkl}, ...) = E^0 - \mu_i F_i - (^1/_3)\Theta_{ij}F_{ij} - (^1/_{15})\Omega_{ijk}F_{ijk} - (^1/_{105})\Phi_{ijkl}F_{ijkl} + ... \quad (1)$$

where F_i, F_{ij}, and so forth, are the electric field, electric field gradient, and so forth, at the origin. E^0, μ_i, Θ_{ij}, Ω_{ijk}, and Φ_{ijkl} are the energy and the dipole, quadrupole, octopole, and hexadecapole moment of the free molecule, respectively. The subscripts denote the Cartesian components, and the repeated subscript implies summation over x, y, and z. In the present work, the traced quadrupole moment[22−24] has been calculated instead of the traceless quadrupole moment of Buckingham.[20] The calculated electric moments reported in this work are evaluated at the center of mass of each molecule which allows comparison at equal footing.

The components of Θ and Ω at the ground state of a molecule can be related to the corresponding dipolar polarizability tensors α and β through the use of the sum-over-states (SOS) expressions[25,26] under closure approximation. The evaluation of the axial component of static α in the SOS formulation needs the transition energy ($\Delta E = \hbar\omega_{mg}$) and the transition dipole moment between the ground and excited states, ($\mu_{gm} = \langle g|x|m\rangle$).

$$\alpha_{xx} = \frac{2e^2}{\hbar}\sum_{m\neq g}\frac{\mu_{gm}\mu_{mg}}{\omega_{mg}} \quad (2)$$

Likewise, the axial component of the static β can be calculated from the electronic properties of excited states. For the two-photon SOS term,

$$\beta_{xxx} = \frac{6e^3}{\hbar^2}\sum_{m,n\neq g}\frac{\mu_{gm}\mu_{mn}\mu_{ng}}{\omega_{mg}\omega_{ng}} \quad (3)$$

Equations 2 and 3 can be simplified with the introduction of an average $\Delta E = \hbar\omega$ (closure approximation). The linear polarizability can now be written as

$$\alpha_{xx} = \frac{2e^2}{\hbar\omega}\sum_{m\neq g}\langle g|x|m\rangle\langle m|x|g\rangle \quad (4)$$

Using the projection operator defined over the state vectors, $\hat{O} = \sum_m |m\rangle\langle m| = 1$, and noting $\langle g|x|g\rangle = 0$, eq 4 can be written as

$$\alpha_{xx} = \frac{2e^2}{\hbar\omega}\langle g|x^2|g\rangle \quad (5)$$

Exactly in a similar manner, eq 3 can be recast into the following form:

$$\beta_{xxx} = \frac{6e^3}{\hbar^2\omega^2}\langle g|x^3|g\rangle \quad (6)$$

The integrals appearing in eqs 5 and 6 are the axial component of Θ and Ω at the ground state of a molecule. The components of each multipole moment are calculated by the analytical evaluation of appropriate energy derivatives. With an increase in polarization as the size of the molecule increases, both the electric moments and polarizabilities should increase. However, the higher-order properties should be much more sensitive in this respect. The electric moments reported here are obtained by using the following expressions which are analogous to those used for dipolar polarizabilities.[27]

The mean quadrupole moment:

$$\Theta = {}^1/_3(\Theta_{xx} + \Theta_{yy} + \Theta_{zz}) \quad (7)$$

The vector part of octopole moment:

$$\Omega = (\Omega_x{}^2 + \Omega_y{}^2 + \Omega_z{}^2)^{1/2} \quad (8)$$

where $\Omega_i = \Omega_{iii} + \Omega_{ijj} + \Omega_{ikk}$, $i, j, k \in (x, y, z)$. At the ground state, the electric properties have been calculated at the HF level from the SCF density matrix and at the MP2 level from the generalized MP2 density matrix.[28] The multipole moments of excited states have been calculated from the corresponding relaxed generalized CI density[29] obtained from the solution of appropriate CPHF equations.

To compare the pattern of charge transfer between the molecules, we have calculated atomic charges in the ground and excited states by using the natural population analysis (NPA) scheme.[30] For each conformation at the ground state, NPA atomic charges are calculated from the MP2 density matrix at the MP2/6-31+G**//HF/6-31+G** level. For the excited states, the NPA atomic charges are calculated from the corresponding relaxed density matrices[29] constructed from the CIS calculation. The NPA charge transfer obtained in MP2 calculation should

TABLE 1: Equilibrium Inter-Ring Bond Length, Electric Moments, Average BLA Parameter, Hardness Parameter, and Relative Energy for Molecule I at the Planar and Orthogonal Ground State

	$\phi_{7-1-8-9} = 0°$		$\phi_{7-1-8-9} = 90°$		$\phi_{7-1-8-9} = 180°$	
	HF	MP2	HF	MP2	HF	MP2
$r_{(C1C8)}$ (Å)	1.378	1.407	1.473	1.438	1.382	1.410
μ (D)	11.61	12.46	22.86	17.13	13.20	13.97
Θ (D-Å)	−95.5	−94.9	−91.6	−93.5	−93.9	−93.0
Ω (D-Å^2)	331.08	349.22	578.13	426.02	407.30	429.86
δr (Å)	0.104	0.061	0.014	0.034	0.100	0.058
η (eV)	3.893		3.263		3.829	
E_{rel}[a] (eV)	0.000	0.000	1.026	0.846	0.024	0.054

[a] The absolute energy (au) at $\phi_{7-1-8-9} = 0°$ is −718.702 23 (HF/6-31+G**)/−721.01234 (MP2/6-31+G**).

TABLE 2: Equilibrium Inter-Ring Bond Length, Electric Moments, Average BLA Parameter, Hardness Parameter, and Relative Energy for Molecule II at the Planar and Orthogonal Ground State

	$\phi_{7-1-8-9} = 0°$		$\phi_{7-1-8-9} = 90°$		$\phi_{7-1-8-9} = 180°$	
	HF	MP2	HF	MP2	HF	MP2
$r_{(C1C8)}$ (Å)	1.350	1.388	1.375	1.434	1.349	1.387
μ (D)	6.835	4.873	5.581	3.827	6.201	4.373
Θ (D-Å)	−94.3	−97.7	−97.3	−97.9	−95.3	−97.8
Ω (D-Å^2)	236.74	561.40	183.47	144.17	218.95	501.91
δr (Å)	0.133	0.084	0.128	0.060	0.134	0.084
η (eV)	4.048		3.633		4.059	
E_{rel}[a] (eV)	0.005	0.002	1.669	1.085	0.000	0.000

[a] The absolute energy (au) at $\phi_{7-1-8-9} = 180°$ is −718.694 92 (HF/6-31+G**)/−721.00136 (MP2/6-31+G**).

not be compared with the corresponding CIS calculated results. The charge transfer quantity obtained for the ground and excited states can give a qualitative picture to distinguish the pattern of conformation dependence of polarity of the states between the isomers.

2.2. Calculations Using the Solvent. The solvent effect at the planar and orthogonal ground state of the molecules has been calculated by employing the recent variant of the polarizable continuum model (PCM) of solvent called the conductor-like PCM[18,19] at the HF/6-31+G** level. The detailed procedure describing the CPCM and its latest improvements can be found in the literature.[19] In the present calculation, the average area of tesserae taken over each sphere in the cavity surface is about 0.2 Å^2. The polarized solute−solvent interaction[31−33] within the CPCM considers the geometry relaxation of solute in equilibrium with the solvent reaction field. Since the present molecules possess a significant dipole moment at the ground state, the calculated electrostatic solute−solvent interaction energy is taken as the solvation energy. The latter has been estimated as the difference between the solvent-polarized HF energy and the gas phase HF energy each of which has been calculated at the respective equilibrium geometry. The non-electrostatic contributions to the molecular free energy in solution comprised of dispersion,[34] repulsion,[34] and cavitation energies (using the Pierotti−Claverie formula)[35,36] have been calculated with classical procedures. For the present molecules, it has been noted that for a given solvent dispersion energy, in general, balances the energy expended in the cavity formation. The solvent-modified transition energy and the spectroscopic properties for vertical excitations are calculated by using the CPCM in the framework of CIS calculations[37] at the solvent-modified geometry of each molecule. All calculations have been carried out using the Gaussian 03 package.[38]

3. Results and Discussion

3.1. Ground State Electronic Structure and Properties. The HF/6-31+G** and MP2/6-31+G** calculated equilibrium inter-ring bond lengths along with electric multipole moments of molecules obtained at different inter-ring torsion angles (ϕ) are presented in Tables 1 and 2. The other equilibrium bond lengths and bond angles are given in the Supporting Information. Since the BLA parameter can satisfactorily account[39,40] for the extent of polarization, the average value of BLA parameter (δr) of the two rings calculated as the difference between the average CC single and double bond lengths is also included in Tables 1 and 2. Another useful quantity which can also account for the extent of polarization due to CT interaction is the hardness parameter (η) which has been calculated from the lowest unoccupied molecular orbital (LUMO)−highest occupied molecular orbital (HOMO) energy gap as $\eta = {}^1/_2(\epsilon_{LUMO} - \epsilon_{HOMO})$.[41] In the single transition approximation, for the closed-shell case, η can be related to the vertical transition energy (ΔE) corresponding to the HOMO (φ_i) → LUMO (φ_j) excitation as

$$2\eta = \Delta E + J_{ij} - 2K_{ij} \tag{9}$$

The last two terms in eq 9 refer to two-electron repulsion and exchange integrals, respectively. In general, the smaller δr and η correspond to stronger polarization[40] arising from the longitudinal CT interaction.

The relative ease of polarization of the two molecules on going to 90° can be understood by comparing the lowering of their δr values which is ∼86.5%/∼44.3% for **I** and ∼4%/∼28.6% for **II** at the HF/MP2 level. As expected, both the C-donor and C-acceptor bond lengths of **I** have been found to decrease significantly on twisting. In contrast, these bond lengths in **II** remain almost unchanged. It has been noted that the inclusion of EC shifts the CC single bond lengths of **I**/**II** by ∼ −(0.01−0.02) Å/∼ −0.02 Å at $\phi = 0°$ and ∼ +(0.02−0.05) Å/∼ −(0.02−0.045) Å at $\phi = 90°$ and CC double bond lengths by ∼ +0.03 Å/∼ +0.03 Å at $\phi = 0°$ and ±(0.004−0.035) Å/∼ +(0.035−0.06) Å at $\phi = 90°$. The EC causes appreciable shortening of the C-acceptor bond (by 0.02 Å) and elongation of the C-donor bond (by 0.03 Å) in the twisted structure of **I**. In contrast, the corresponding bond lengths (increased by ∼0.01 Å in both conformations) of molecule **II** are less sensitive to EC. It should be noted that the effect of EC on the inter-ring bond distance (r_{C1C8}) in the twisted conformers of **I** and **II** shows a markedly different trend. In the former, r_{C1C8} decreases by 0.035 Å, while, in the latter, it increases by 0.06 Å. The calculated bond lengths of two molecules obtained for $\phi = 0$ and 180° at a given level showed no noticeable difference.

Regarding the bond angles, it has been noted (see Tables 1 and 2 in the Supporting Information) that the values predicted at the HF and MP2 calculations differ mostly by 2−3°. Here, we mention some important MP2 calculated torsion angles. The torsion angles, $\phi_{4-5-16-17}$ (19.6°/ 17.4°) for **I** and $\phi_{9-10-13-14}$ (20.7°/ 10.7°) for **II** at 0°/90° confirm that the NH_2 group prefers to remain out of plane with the attached ring. For both molecules, the smaller ring at $\phi = 90°$ is not planar, as indicated by $\phi_{1-8-9-10}$ which is 27.5° for **I** and 27.7° for **II**.

Our calculated δr values indicate invariably much stronger polarization in molecule **I** (Table 1) compared to molecule **II** (Table 2) at 90°. It will be interesting to compare the relative ease of ground state polarization of isomers **I** and **II** with the unsubstituted sesquifulvalene. The MP2/6-31+G** calculated r_{C1C8} and δr values for the planar (orthogonal) conformer are 1.407 and 0.061 Å (1.438 and 0.034 Å) for **I**, 1.388 and 0.084 Å (1.434 and 0.060 Å) for **II**, and 1.397 and 0.068 Å (1.442

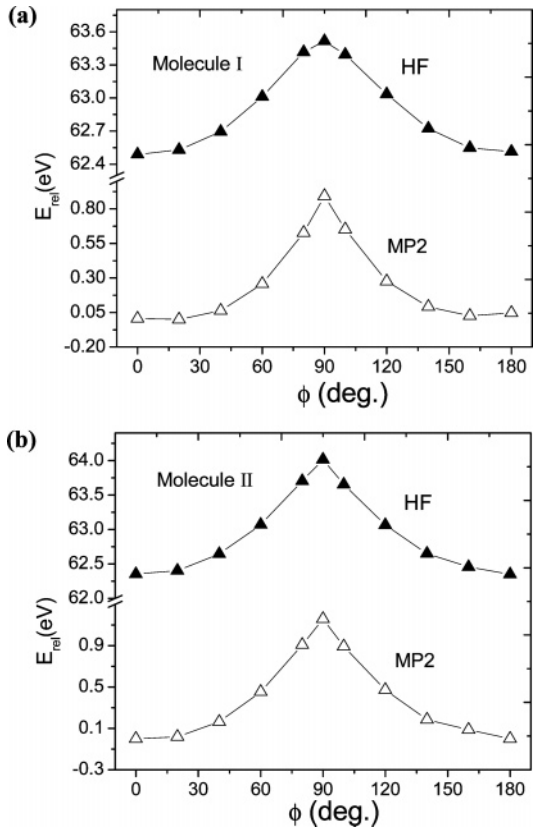

Figure 1. Plot of the relative energy curve at the ground state for different inter-ring torsion angles for (a) molecule **I** and (b) molecule **II**. Here, MP2 refers to the single point electronic energy obtained at the HF/6-31+G** geometry.

and 0.005 Å) for sesquifulvalene.[17] At the planar geometry, the extent of polarization in **I** is greater than that of isomer **II** and sesquifulvalene. However, at 90°, the relative order of polarization is sesquifulvalene hydrocarbon > **I** > **II** which indicates that in the presence of substituents the longitudinal CT significantly reduces the ring aromaticity in both **I** and **II**. The relatively stronger CT interaction in **I** compared to **II** is also indicted by our calculated η values.

At the ground state, the lowest energy structure is predicted at $\phi = 0°$ for molecule **I** (Table 1) and $\phi = 180°$ for molecule **II** (Table 2). The energy difference (in kcal/mol) between the two planar conformers ($\phi = 0$ and 180°) of two molecules at the MP2 level is 1.24 (**I**) and 0.05 (**II**). The relative energy of each molecule (with respect to the most stable conformer at MP2) obtained in the HF and single point MP2 calculations has been plotted against ϕ in Figure 1. The energy curves are fairly symmetric around the maximum at $\phi = 90°$. The planar ($\phi = 0°$) → orthogonal barrier height (kcal/mol) at the HF (MP2) level is 23.7 (20.4) for **I** and 38.4 (26.7) for **II**. However, the inclusion of EC at the ground state geometry results in slightly lowering of the energy barrier 19.5 for **I** and 25.0 for **II** with a difference of 5.5 which may reasonably account for the greater ease of polarization of **I** on twisting.

The difference in polarization between the two molecules especially at $\phi = 90°$ is expected to have a significant effect on their charge distribution which in turn should be reflected in the electric properties. The calculated ground state electric moments of **I** when plotted against ϕ sharply peak at 90° (Figure 2a,b) which can be ascribed to the phenomenon of sudden polarization. This result is fairly consistent with that obtained by Ratner et al.[13] for 4-quinopyran molecules. Here, we would like to mention that in the case of charge asymmetric polyenes the phenomenon of sudden polarization was noted[11,12] for the excited states only. In contrast, molecule **II** shows (Figure 2c,d) sharp depression in higher moments at $\phi = 90°$. This markedly opposing trend in the electric moments may be attributed to the inter-ring CT which enhances the longitudinal CT in **I** and lowers it in **II**.

It can be seen that EC has a significant effect on the electric properties. The incorporation of EC substantially changes the dipole and octopole moments of molecule **II** in comparison to **I**. It will be interesting to examine whether this very difference in the polarity between the molecules at the ground state can also be reflected in their excited state electric and spectroscopic properties.

3.2. Low Lying Excited States and Their Electric Properties in the Gas Phase. The relative energy curves of four low lying excited singlet states of molecules **I** and **II** are plotted in Figure 3. The curves, in general, are symmetric around 90°. In our subsequent discussions, we shall refer to the planar conformation as the one with $\phi = 0°$ and report the barrier height or relative energy differences in kilocalories per mole. For the S_1 state of **I**, the maximum (above the planar conformer by 3.4) occurs at 90°. The S_2 curve has a shallow minimum at 40° with an energy 1.3 lower than its planar conformer which is followed by a sharp maximum at 90° (16.1 above the minimum). The S_3 state predicts a deep minimum at 90° which lies below its planar conformer by about 17.3. The energy curve of the S_4 state passes through a shallow minimum (0.3) at 20° and a maximum (10.8) at 90° with respect to the planar structure. It should be noted that the incorporation of EC (MP2/6-31+G**//HF/6-31+G**) lowers Δh (Table 3) of each state by about 3.0.

We have noted that the inclusion of EC (at the MP2 level) in the ground state at $\phi = 180°$ (Figure 3a) is necessary to obtain the same energy ordering of S_2 and S_4 states of **I** as predicted for $\phi = 0°$ with and without EC. The calculated barrier height of the S_3 state after including EC at $\phi = 0$ and 90° results in a barrier height of 3.3 in contrast to the negative value (Table 3). The relative order of stability of the S_0 and S_3 states, however, is not altered with and without inclusion of EC in the ground state. Considering the MP2/6-31+G** calculated ground state energy of **I** with HF (MP2) geometry, it is confirmed that at the planar/orthogonal structure the S_3 state lies above the S_0 state by 97.0 (88.8)/59.3 (62.2). The increase in Δh for this state is also noted in solvents with an increase in polarity. The modified Δh values of the S_1 (2.5) and S_2 (13.6) states are fairly comparable to the values (3.4 and 14.8) in Figure 3a.

The pattern of energy curves of the low lying excited singlets of molecule **II** (Figure 3b) differ rather markedly from that obtained for **I**. Here, no crossing in the energy curve is noted. Except for the S_1 state, the remaining curves are symmetric around 90°. All of the PE curves pass through a maximum at 90° with widely varying energy barriers (Table 3). The ease of twisting is highest in the S_3 state for which Δh (15.6 (HF) and 3.9 (MP2)). The effect of EC on Δh for the other excited states is also rather significant, each lowered by about 12.0.

It is interesting to note (Table 3) that the barrier height of the excited states (Δh_n) is significantly smaller than the ground state (Δh_0) of each molecule. This results in lowering of the transition energy (ΔE_n) of an excited state, S_n, on going from the planar to the orthogonal structure. For both molecules, we have noted that ΔE_n^{ϕ} ($0^0 < \phi \leq 90°$) is always lower than ΔE_n^{0} in a vacuum due to $\Delta h_n^{\phi} < \Delta h_0^{\phi}$ (eq 10). This general trend

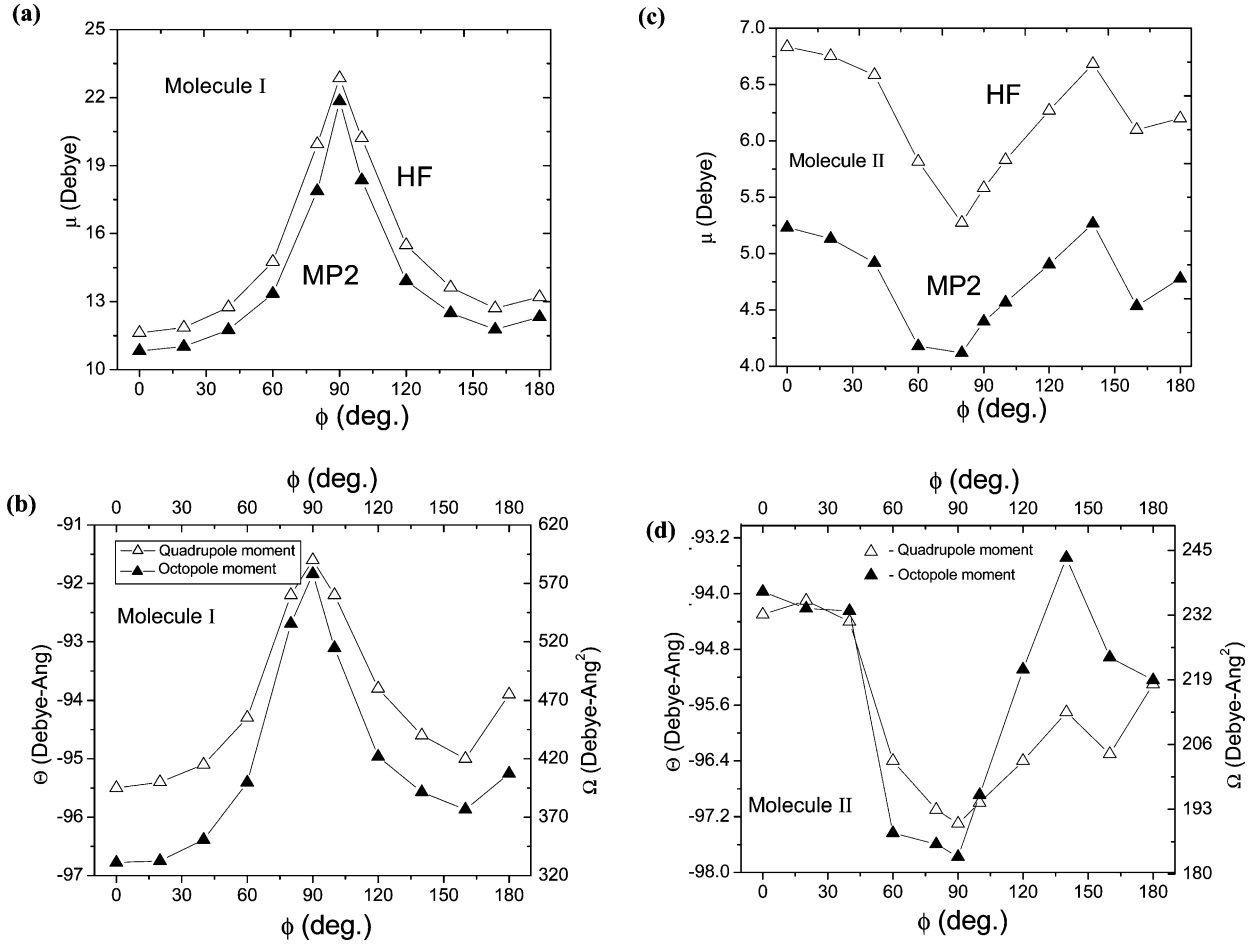

Figure 2. Variation of the HF/6-31+G** calculated (a) dipole moment, (b) quadrupole and octopole moment at the ground state of molecule **I** against the inter-ring torsion angle. Parts c and d show similar plots of the electric multipole moments for molecule **II**.

obtained here is fairly consistent with the earlier theoretical studies.[12,13]

$$(\Delta E_n^{\phi} - \Delta E_n^{0}) = (\Delta h_n^{\phi} - \Delta h_0^{\phi}) < 0 \qquad (10)$$

Let us now see the pattern of variation of electric moments with ϕ for molecules **I** and **II** in different excited states. Since we have noted the importance of EC for molecule **I** at $\phi = 180°$ to obtain the correct energy ordering, the electric moments and charges for this molecule in the excited states have been calculated using the corresponding modified ground state geometry and the results are included in the subsequent figures. The similar electron correlation correction at $\phi = 0$ and 90° does not change the relative order of polarity of the states. It can be seen from Figure 4a,b the S_4 and S_5 states of **I** depict the highest value of electric moment at 90° with sharp peaks. The S_1 state in this respect show a minimum, while the S_2 and S_3 states exhibit rather smooth variation. The pattern of variation of electric moments of molecule **I** resembles those of push−pull substituted polyenes which showed sudden polarization in the lower lying excited states. In contrast, the dipole moment (Figure 4c) and other higher moments (not shown here) of molecule **II** in the low lying excited states do not exhibit any sudden rise at $\phi = 90°$. The highest electric moments of the S_1 state of both molecules at $\phi = 0°$ may lead to a positive solvatochromic effect.

The marked difference in the conformation dependence of polarization and electric moments of the two molecules can be rationalized in terms of the longitudinal CT across the rings. For this purpose, we have calculated the net amount of charge ($\sum q$) by summing the NPA atomic charges over the seven-membered ring along with the attached substituent for each molecule. From the sign and magnitude of $\sum q$, the direction and also the extent of CT can be interpreted. The calculated $\sum q$ quantities are plotted against ϕ (Figure 5) for the ground and low lying excited states of each molecule. The S_0, S_4, and S_5 states of **I** (Figure 5a) show the sudden increase of donor → acceptor charge transfer at 90°, while the S_2 and S_3 states exhibit rather smooth variation in this respect. The considerable lowering of polarity in the S_1 state of **I** at 90° arises from the LUMO (smaller ring) → HOMO (larger ring) charge transfer. In the case of molecule **II** except for the S_3 state (Figure 5b), the larger ring → smaller ring CT is rather aprreciable for the remaining states at 90°. Thus, the polarity difference between the two molecules especially at 90° arises from the relative contribution of the two kinds of charge transfer. The inter-ring CT, in general, strongly favors the longitudinal CT in **I** and reduces it in **II**.

3.3. Comparison of the Second-Order NLO Property of Molecules. It has so far been discussed that molecule **I** showed sudden polarization in S_0 and S_4 and S_5 states and is thus expected to give an enhanced NLO response (see eq 6) compared to molecule **II**. However, it is a computationally difficult task to obtain NLO properties in the excited state of a molecule. Our analytically calculated components of β along with the average α [$(\alpha_{xx} + \alpha_{yy} + \alpha_{zz})/3$] obtained at the MP2/

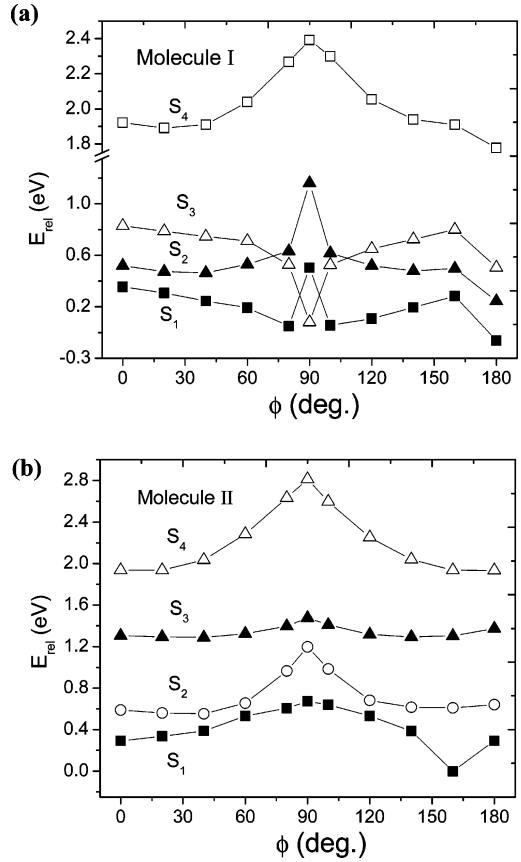

Figure 3. Plots of the relative energy curves of the four low lying singlet excited states against the inter-ring torsion angle for (a) molecule **I** and (b) molecule **II**. The lowest energy of state with the MP2/6-31+G**//HF/6-31+G** calculated ground state is taken as zero.

TABLE 3: (Planar − Orthogonal) Barrier Height (Δ*h*, kcal/mol) for the Ground State (S_0) (Calculated at the HF/6-31+G Level) and Low Lying Excited Singlet States (S_n) (the Total Energy at a Given Conformation = the CIS/6-31+G** Calculated Transition Energy + the HF/6-31+G** Calculated Ground State Energy) in the Gas Phase and Solution**

	molecule **I**				molecule **II**			
S_n[a]	$\epsilon = 1.0$	4.9	20.7	78.4	1.0	4.9	20.7	78.4
S_0	23.7	11.2	8.8	6.0	38.4	38.8	38.9	39.1
S_1 (56 → 57)	6.6	28.1	32.7	25.8	20.5	21.7	22.2	22.6
S_2 (56 → 58)	18.0	28.8			25.7	26.7	26.9	27.6
S_3 (55 → 57)	−14.1	−3.0	−0.16	6.6	15.6	15.8	15.9	16.1
S_4 (56 → 59)	14.0				31.9	32.7	33.0	33.5

[a] The most dominant one-particle excitation characterizing the excited state is given in parentheses. 56 = HOMO, and 57 = LUMO.

6-31+G**//MP2/6-31+G** level for the ground state of each molecule are given in Table 4. The analytical calculated results of polarizabilities have been found to be identical to the finite field values. The nonzero vector components of β of both molecules arise from the nonzero dipole components. Thus, the quantity β_{vec}[27] $[(\beta_x\mu_x + \beta_y\mu_y + \beta_z\mu_z)/|\mu|$ with β_i $(i = x, y, z) = \beta_{iii} + \beta_{ijj} + \beta_{ikk}$ $(i \neq j \neq k)]$ which refers to the vector part of β projected along the molecular dipole moment is more appropriate and is given in the table for the sake of comparison. Both α and β_{vec} increase with an increase in the extent of polarization of molecules (Tables 1 and 2), although the variation of α is rather small. For each molecule, polarizabilities attain the highest values at 90°. The rather large enhancement of β_{vec} for **I** (208.3×10^{-30} esu) in comparison to **II** (57.0×10^{-30} esu) can be ascribed to its sudden polarized ground state.

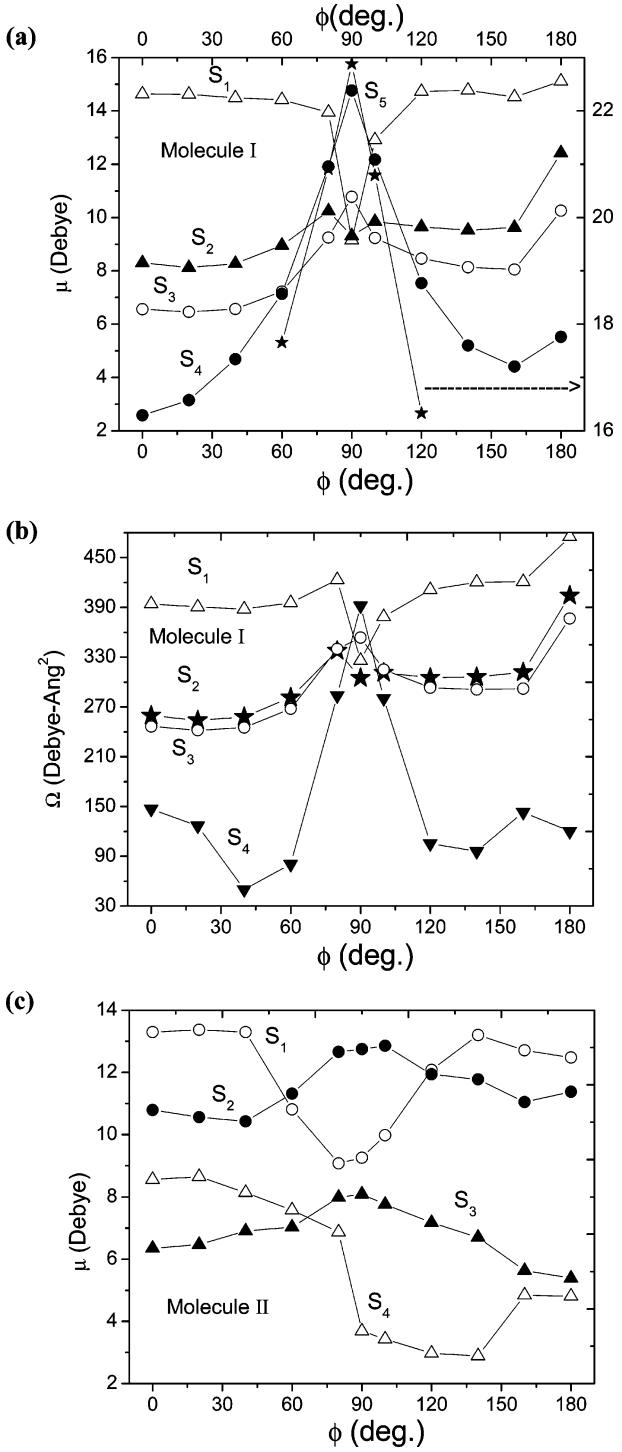

Figure 4. Variation of the CIS/6-31+G** calculated (a) dipole moment (the dotted arrow points to the right axis for the S_5 state), (b) octopole moment of low lying excited singlet states of molecule **I** against the inter-ring torsion angle. (c) A similar plot of the dipole moment for molecule **II**.

To rationalize the second-order polarizability, the state-wise contributions of excited states calculated by using the following two-state expressions[42,43] (eq 11) are also given in Table 4. To obtain a precise estimate of β in the SOS method at the CI level, it requires one to consider many excited states incorporating single and double excitations in CI calculations which is a huge computational task. However, to compromise the computational cost and accuracy, MP2 results are useful. In view of the earlier theoretical investigation,[17] the present CIS/6-

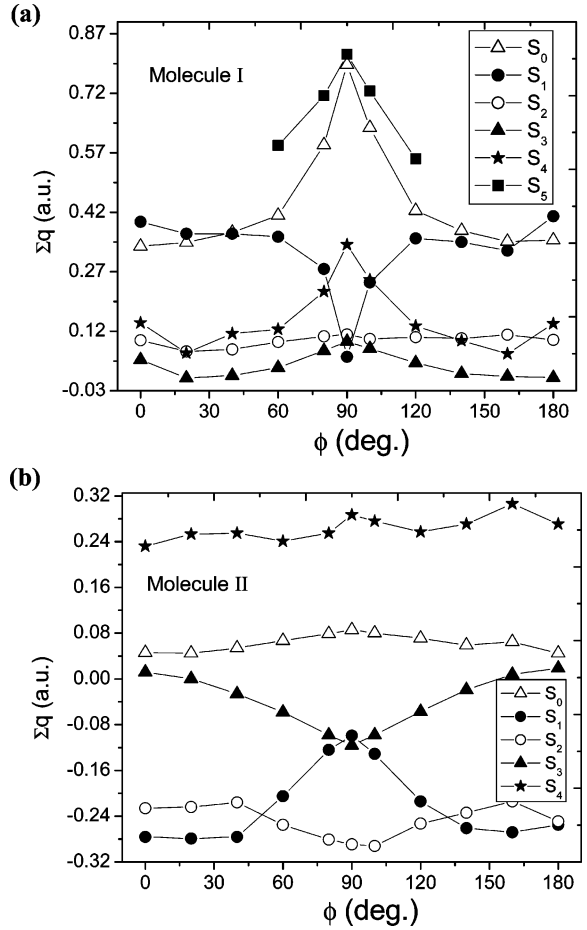

Figure 5. Plots of the net charge on the donor part for the ground (estimated from the NPA charges calculated at the MP2/6-31+G** level) and low lying excited singlet states (estimated from the NPA charges calculated at the CIS/6-31+G** level) against the inter-ring torsion angles for (a) molecule **I** and (b) molecule **II**.

TABLE 4: Static Linear (α in 10^{-23} esu) and Quadratic Polarizabilities (β in 10^{-30} esu) at the Ground State of Molecules in a Vacuum

	molecule **I**		molecule **II**	
	$\phi = 0°$	$\phi = 90°$	$\phi = 0°$	$\phi = 90°$
		MP2/6-31+G**		
α	3.472	3.630	2.977	3.132
β_x	−75.02	−129.91	17.64	−59.11
β_y	−4.03	18.95	4.85	13.62
β_z	−0.52	−17.56	9.29	−55.78
β_{vec}	−78.80	129.46	−17.04	39.95
		state-wise contribution (β)		
S_1	36.433	−7.453	11.797	40.594
S_2	−4.623	−8.563	9.434	2.199
S_3	−0.350	−41.122	−6.192	11.536
S_4	−0.096	−0.434	0.008	−0.051
S_5[a]	0.661	0.032		

[a] Since the S_5 (54 → 57) state appears at 60°, the quantities reported for this state refer to this conformation. Polarizability units: α, 1 au = 1.4817×10^{-25} cm^3; β, 1 au = 8.6392×10^{-33} cm^4 statvolt^{-1}.

31+G** calculated results of two-state β[42,43] can give only a qualitative picture.

$$\beta = 6\frac{\mu_{ge}^{\ 2}\Delta\mu}{\Delta E_{ge}^{\ 2}} = 9\frac{f_0\Delta\mu}{\Delta E_{ge}^{\ 3}} \qquad (11)$$

In the above equations, μ_{ge}, $\Delta\mu$, and ΔE_{ge} refer to the transition moment, the difference in dipole moment, and the transition energy between the ground and excited state, respectively. The oscillator strength is $f_0 = (^2/_3)\mu_{ge}^{\ 2}\Delta E_{ge}$. The state-wise contribution of β depends on the spectroscopic properties of excited states (Table 6). The negative β mainly arises from the excited states of **I** because of its sudden polarized ground state which invariably predicts $\Delta\mu < 0$. For both molecules, the contributions of β from each state appreciably increase on going to 90° because the most sensitive term ΔE_{ge} decreases considerably on twisting (eq 10). The overall change in β on twisting is about 90×10^{-30} esu for **I** and about 39×10^{-30} esu for **II**. Thus, the two-state model qualitatively predicts the same trend in β as obtained in MP2.

TABLE 5: Solvation Energy (ΔE_{pol}, eV), Net Non-Electrostatic ($\Delta E_{non\text{-}elec}$) Energy, Inter-Ring Bond Length (r_{C1C8}, Å), Electric Moments, Average BLA Parameter, and Hardness Parameter (See Units in Table 1) for the Planar and Orthogonal Ground States in Solution

	molecule **I**					
	planar			orthogonal		
	$\epsilon = 4.9$	20.7	78.4	4.9	20.7	78.4
ΔE_{pol}	−9.26	−12.18	−22.04	−21.7	−27.07	−39.69
$\Delta E_{non\text{-}elec}$	1.99	0.62	4.16	2.46	1.10	4.82
$r_{(C1C8)}$	1.412	1.428	1.454	1.487	1.489	1.492
δr	0.07	0.055	0.033	0.005	0.005	0.004
η	3.766	3.782		3.800	3.957	4.221
μ	19.1	22.1	27.3	29.0	30.4	32.95
Θ	−102.4	−103.3	−104.9	−106.7	−107.6	−109.5
Ω	967.9	1045.2	1184.2	1219.8	1269.3	1360.8
	molecule **II**					
	planar			orthogonal		
	$\epsilon = 4.9$	20.7	78.4	4.9	20.7	78.4
ΔE_{pol}	−5.61	−6.83	−13.11	−5.12	−6.25	−12.32
$\Delta E_{non-elec}$	2.11	0.73	4.29	2.30	0.94	4.53
r_{cc}	1.350	1.350	1.351	1.375	1.374	1.375
δr	0.133	0.133	0.132	0.128	0.129	0.128
η	3.987	3.965	3.942	3.616	3.609	3.597
μ	8.1	8.4	8.9	6.7	7.3	7.3
Θ	−97.8	−97.8	−97.8	−99.2	−99.4	−99.5
Ω	657.8	668.7	689.9	538.9	562.8	559.3

3.4. Solvent Effect on the Ground State Structure and Energy. The calculated solvation energy, net non-electrostatic energy along with the inter-ring bond distance, BLA parameter, hardness parameter, and electric moments of molecules **I** and **II** are presented in Table 5. It is important to note that although the solvation energies of the isomers differ appreciably the corresponding net non-electrostatic energies are rather comparable. Compared to the HF/6-31+G** calculated gas phase results (Table 1), the $r_{cc}/\delta r$ value of **I** at 0° (90°) increases/decreases by 0.03 Å/0.03 Å (0.01 Å/0.01 Å) in chloroform through 0.05 Å/0.05 Å (0.015 Å/0.01 Å) in acetone to 0.075 Å/0.07 Å (0.02 Å/0.01 Å) in water. Except for Θ, the other moments of **I** increase with an increase in solvent polarity, and for a given solvent, these are fairly large at $\phi = 90°$. The larger polarization in conjunction with appreciable lowering of barrier height (Table 3) in solvents confirms that molecule **I** is highly ionic in the twisted conformer. All of these facts lend support to the sudden polarization of **I** in the ground state. The solvent shift of η (Table 1) indicates that ΔE (eq 9) for the $S_0 \rightarrow S_1$ transition in **I** is expected to be red-shifted (blue-shifted) in the planar (orthogonal) geometry.

In contrast, molecule **II** resists polarization in solution as shown by a rather insignificant change in electric moments (except for Ω) and structural parameters (compared to the results in Table 2) even in the presence of highly polar solvent. This

TABLE 6: Solvent-Free and Solvent-Induced Dipole Moment (μ, D), Oscillator Strength (f_0, in 10^{-1} au), Transition Frequency (ΔE, in 10^2 cm^{-1}) in a Vacuum, and Solvent-Induced Shift in Transition Frequency ($\Delta\epsilon$, in 10^2 cm^{-1}) for the Low Lying Excited Singlet States (S_n) in the Planar and Orthogonal Structures

molecule **I**

(planar geometry)

	$\epsilon = 1.0$			4.9			20.7			78.4		
S_n	μ	ΔE	f_0	μ	$\Delta\epsilon$	f_0	μ	$\Delta\epsilon$	f_0	μ	$\Delta\epsilon$	f_0
S_1	14.1	301.0	12.2	18.9	−22.2	11.9	20.2	−22.3	11.4	23.1	−8.1	10.3
S_2	7.8	314.3	1.16	12.6	22.6	0.60	15.1	8.5	0.52	20.1	28.7	0.46
S_3	6.1	339.3	0.08	10.6	75.8	0.02	13.7	14.1	0.02	22.4	30.7	0.64

(orthogonal geometry)

	$\epsilon = 1.0$			4.9			20.7			78.4		
S_n	μ	ΔE	f_0	μ	$\Delta\epsilon$	f_0	μ	$\Delta\epsilon$	f_0	μ	$\Delta\epsilon$	f_0
S_1	8.6	241.5	0.23	12.2	96.6	0.44	17.2	121.0	1.90	22.6	120.7	1.93
S_2	8.8	294.6	0.48	20.0	83.4	4.10						
S_3	10.3	207.3	0.90	13.1	89.9	0.04	14.8	114.9	0.03	30.7	164.8	6.86

molecule **II**

(planar geometry)

	$\epsilon = 1.0$			4.9			20.7			78.4		
S_n	μ	ΔE	f_0	μ	$\Delta\epsilon$	f_0	μ	$\Delta\epsilon$	f_0	μ	$\Delta\epsilon$	f_0
S_1	12.8	291.4	1.51	15.4	−4.2	1.80	15.7	−6.5	1.85	16.4	−7.0	2.10
S_2	10.3	315.4	2.65	12.2	−2.7	2.41	12.5	−3.6	2.38	13.0	−3.5	2.33
S_3	5.8	373.2	10.0	7.0	1.5	10.3	7.4	1.6	10.3	8.0	1.4	10.2
S_4	8.1	424.1	0.02	8.2	5.9	0.04	8.3	6.2	0.05	8.6	4.5	0.06

(orthogonal geometry)

	$\epsilon = 1.0$			4.9			20.7			78.4		
S_n	μ	ΔE	f_0	μ	$\Delta\epsilon$	f_0	μ	$\Delta\epsilon$	f_0	μ	$\Delta\epsilon$	f_0
S_1	8.8	228.8	4.73	10.9	−1.7	4.66	11.2	−2.3	4.65	11.7	−2.5	4.75
S_2	12.3	271.2	0.02	15.0	−1.0	0.27	15.2	−1.7	0.28	15.7	0.4	0.33
S_3	7.6	293.6	4.49	8.8	0.3	4.65	9.0	0.5	4.69	9.4	0.4	4.61
S_4	3.2	401.6	0.04	1.5	7.0	0.04	1.7	8.0	0.04	2.3	7.3	0.04

has also been reflected in the larger barrier height (Table 3). The decrease in polarity of molecule **II** at 90° (μ and Ω are lowered by about 18% in both vacuum and solution) indicates its greater covalent character which may arise from the greater inter-ring CT which almost balances the donor → acceptor CT. The solvent-modified η shows that the lowest energy transition in **II** should be red-shifted in polar solvents.

3.5. Influence of Solvent on the Energy and Electronic Properties of Low Lying Excited States. The influence of solvent on the planar → orthogonal energy barrier (Δh) of the molecules in different electronic states is given in Table 3. Note that the S_4 (56 → 59) and S_5 (54 → 57) states of **I** showing sudden polarizations in a vacuum do not appear in the solution phase. In contrast to the S_0 state, the S_1 state of **I** having higher μ (by 5.5 D in a vacuum) at $\phi = 0°$ compared to that at $\phi = 90°$ (Figure 4a) results in an appreciably large increase of Δh in the presence of solvent (Table 3). However, the solvent dependence of Δh of an excited state, in general, does not follow the polarity difference between the planar ($\phi = 0°$) and twisted ($\phi = 90°$) conformers. For an excited state, S_n, the change in barrier height [$\Delta h'(\epsilon) = \Delta h(\epsilon > 1) - \Delta h(\epsilon = 1)$] due to solvent depends explicitly on the following three terms.

$$\Delta h'(\epsilon) = [\Delta\epsilon^{90}(S_0) - \Delta\epsilon^{0}(S_0)] + [\Delta E^{90}(\epsilon > 1) - \Delta E^{90}(\epsilon = 1)] - [\Delta E^{0}(\epsilon > 1) - \Delta E^{0}(\epsilon = 1)] \quad (12)$$

Equation 12 can also be written in an alternative form as

$$\Delta h'(\epsilon) = [\Delta\epsilon^{90}(S_0) - \Delta\epsilon^{0}(S_0)] - [\Delta E^{0}(\epsilon > 1) - \Delta E^{90}(\epsilon > 1)] + [\Delta E^{0}(\epsilon = 1) - \Delta E^{90}(\epsilon = 1)] \quad (13)$$

The first term in eq 12 corresponds to the solvation energy difference between the planar and twisted conformers in the ground state (Table 5), and the second and third terms refer to the solvent-induced transition energy shift [$\Delta\epsilon = \Delta E^{\phi}(\epsilon > 1) - \Delta E^{\phi}(\epsilon = 1)$] of an excited state (Table 6). For molecule **I**, the first term is significantly negative and the absolute value increases with an increase in solvent polarity, while, for **II**, this term is positive but very small. As a result of sudden polarization at $\phi = 90°$, the second term of eq 12 for **I** increases considerably on an increase in solvent polarity due to blue-shift compared to the relatively smaller third term due to either red- or blue-shift at $\phi = 0°$. The last term of eq 13 has reasonably high positive values for both molecules (eq 10). Therefore, for the excited states of **I** having larger $\Delta h'$, the second term is significantly negative. However, the rather smaller value of $\Delta h'$ for the excited states of **II** is accounted for by the red-shift in transition energy (Table 6) on going to 90° in either vacuum or solution which results in almost cancellation of the last two terms in eq 13.

The calculated solvent effects on the electronic properties of the low lying excited states of molecules **I** and **II** are compared in Table 6. It can be seen that, for the excited states of **I**, μ increases significantly with an increase in solvent dielectric which, however, shows rather marginal variation for **II**. This change in μ indicates a much higher polarity of the excited states of **I** compared to **II**. However, for a given solvent, the dipole moment of each excited state of both molecules follows the same trend as has been predicted in a vacuum. This general trend may be attributed to the polarized solute−solvent interaction considered in the present work.

Since the calculated solvation energy includes only the electrostatic contribution, the variation of $\Delta\epsilon$ can be understood qualitatively on the relative values of μ (in a vacuum) between the states S_n and S_0. The red-shift in the planar S_1 state of **I** is thus accounted for by its higher μ compared to S_0. Likewise, the S_1 and S_2 states of **II** at $\phi = 0$ and 90° predict red-shift which is consistent with their relative μ values. Of the two molecules, the more intense red-shifted transition (higher f_0) occurs for **I**. The remaining states of **I** in both conformations possess much smaller μ compared to the S_0 state and thus exhibit blue-shift. The S_3 and S_4 states of **II** show blue-shifted transition in both geometries with $\Delta\epsilon$ being larger for the S_4 state (especially at 90° for which μ has the lowest value (3.2 D) versus the ground state value of 5.6 D in a vacuum).

4. Conclusions

The present investigation considered two structural isomers, **I** and **II**, of identical conjugative length in which the larger and smaller rings act as auxiliary donor (D) and acceptor (A), respectively. It has been demonstrated that molecule **I** with DDAA combination showed sudden polarization in the ground and excited states (S_4 and S_5) while molecule **II** with ADAD array showed no significant change in polarization at 90°. This pattern of polarization in such twisted molecular systems differs markedly from that of the D−A substituted polyenes in which charge asymmetric results in sudden polarization. The relative position of electron transfer groups accounts for the enhanced (D → (D → A) → A)/diminished (A ← (D → A) ← D) CT interaction in **I**/**II** on going from 0 to 90°. These modes of charge transfers have been found to be fairly consistent with the extent of CT across the ring especially at 90°.

The present study on the TICT isomers showed the emergence of large NLO property from the sudden polarized ground state of molecule **I** and also the possibility of evolution of enhanced nonlinearity from its sudden polarized excited states. The present study showed that appropriate modification in the electronic structure of TICT related molecular systems can make them potential NLO-phores.

Since the chosen molecules are appreciably polar and only the dominant solute−solvent electrostatic interaction is considered, the variation of their rotational energy barriers and transition energies in solution can be satisfactorily interpreted and distinguished from each other in terms of the polarity difference between the ground and excited states.

Acknowledgment. We thank the CSIR, Government of India, New Delhi, for financial assistance (Grant No. 01(1930)/04/EMR-II).

Supporting Information Available: Tables showing the HF/6-31+G** and MP2/6-31+G** calculated ground state equilibrium structural parameters for molecules **I** and **II**. This material is available free of charge via the Internet at http://pubs.acs.org.

References and Notes

(1) Dauben, W. G.; Ritscher, J. S. *J. Am. Chem. Soc*. **1970**, *92*, 2925.
(2) Wulfman, C. E.; Kumei, S. E. *Science* **1971**, *172*, 1061.
(3) Salem, L. *Science* **1976**, *191*, 822.
(4) Brooks, B. R.; Schaefer, H. F., III. *J. Am. Chem. Soc.* **1979**, *101*, 307.
(5) Buenker, R. J.; Bonačić-Koutecký, V.; Pogliani, L. *J. Chem. Phys*. **1980**, *73*, 1836.
(6) Petsalakis, I. D.; Thuodorakopoulos, G.; Nicolaides, C. A.; Buenker, R. J.; Peyerimhoff, S. D. *J. Chem. Phys*. **1984**, *81*, 3161.
(7) El-Taher, S.; Hilal, R. H.; Albright, T. A. *Int. J. Quantum Chem*. **2001**, *82*, 245.
(8) Viel, A.; Krawczyk, R. P.; Manthe, U.; Domcke, W. *Angew. Chem., Int. Ed.* **2003**, *42*, 3434.
(9) Bonačić-Koutecký, V.; Bruckmann, P.; Hiberty, P.; Koutecky, J.; Leforestier, C.; Salem, L. *Angew. Chem., Int. Ed. Engl*. **1978**, *14*, 575.
(10) Brunei, M. C.; Duadey, J. P.; Langlet, J.; Malrieu, J. P.; Momic-chioli, F. *J. Am. Chem. Soc*. **1977**, *99*, 3587.
(11) Ramasesha, S.; Albert, I. D. L. *Chem. Phys.* **1990**, *142*, 395.
(12) Albert, I. D. L.; Ramasesha, S. *J. Phys. Chem*. **1990**, *94*, 6540.
(13) Albert, I. D. L.; Marks, T. J.; Ratner, M. A. *J. Am. Chem. Soc.* **1997**, *119*, 3155.
(14) Nandi, P. K.; Mandal, K.; Kar, T. *Theor. Chem. Acc*. **2005**, *114*, 200.
(15) Keinan, S.; Zojer, E.; Bredas, J. L.; Ratner, M. A.; Marks, T. J. *THEOCHEM* **2003**, *633*, 227.
(16) Morley, J. O. *Int. J. Quantum Chem*. **1997**, *61*, 991.
(17) Yang, M.; Jacquemin, D.; Champagne B. *Phys. Chem. Chem. Phys*. **2002**, *4*, 5566.
(18) Barone, V.; Cossi, M. *J. Phys. Chem. A* **1998**, *102*, 1995.
(19) Cossi, M.; Rega, N.; Scalmani, G.; Barone, V. *J. Comput. Chem.* **2003**, *24*, 669.
(20) Buckingham, A. D. *Adv. Chem. Phys*. **1967**, *12*, 107.
(21) McLean, A. D.; Yoshimine, M. *J. Chem. Phys*. **1967**, *47*, 1927.
(22) Logan, D. E. *Mol. Phys.* **1982**, *46*, 271.
(23) Applequist, J. *J. Math. Phys*. **1983**, *24*, 736.
(24) Applequist, J. *Chem. Phys*. **1984**, *85*, 279.
(25) Ward, J. F. *Rev. Mod. Phys*. **1965**, *37*, 1.
(26) Orr, B. J.; Ward, J. F. *Mol. Phys*. **1971**, *20*, 513.
(27) Kanis, D. R.; Ratner, M. A.; Marks, T. *J. Chem. Rev*. **1994**, *94*, 195.
(28) Handy, N. C.; Schaefer, H. F. *J. Chem. Phys*. **1984**, *81*, 5031.
(29) Wiberg, K. B.; Hadad, C. M.; Lepage, T. J.; Breneman, C. M.; Frisch, M. J. *J. Phys. Chem.* **1992**, *96*, 671.
(30) Reed, A. E, Weinstock, R. B.; Weinhold, F. *J. Chem. Phys*. **1985**, *83*, 735.
(31) Tomasi, J.; Persico, M. *Chem. Rev*. **1994**, *94*, 2027 and references therein.
(32) Miertus, S.; Scrocco, E.; Tomasi, J. *Chem. Phys.* **1981**, *55*, 117.
(33) Cammi, R.; Tomasi, J. *J. Comput. Chem*. **1995**, *16*, 1449.
(34) Amovilli, C.; Mennucci, B. *J. Phys. Chem. B* **1997**, *101*, 1051.
(35) Pierotti, R. A. *Chem. Rev*. **1976**, *76*, 717.
(36) Langlet, J.; Claverie, P.; Caillet, J.; Pullman, A. *J. Phys. Chem*. **1988**, *92*, 1617.
(37) Cammi, R.; Mennucci, B.; Tomasi, J. *J. Phys. Chem. A* **2000**, *104*, 563.
(38) Frisch, M. J.; Trucks, G. W.; Schlegel, H. B.; Scuseria, G. E.; Robb, M. A.; Cheeseman, J. R.; Montgomery, J. A.; Vreven, T., Jr.; Kudin, K. N.; Burant, J. C.; Millam, J. M.; Iyengar, S. S.; Tomasi, J.; Barone, V.; Mennucci, B.; Cossi, M.; Scalmani, G.; Rega, N.; Petersson, G. A.; Nakatsuji, H.; Hada, M.; Ehara, M.; Toyota, K.; Fukuda, R.; Hasegawa, J.; Ishida, M.; Nakajima, T.; Honda, Y.; Kitao, O.; Nakai, H.; Klene, M.; Li, X.; Knox, J. E.; Hratchian, H. P.; Cross, J. B.; Adamo, C.; Jaramillo, J.; Gomperts, R.; Stratmann, R. E.; Yazyev, O.; Austin, A. J.; Cammi, R.; Pomelli, C.; Ochterski, J. W.; Ayala, P. Y.; Morokuma, K.; Voth, G. A.; Salvador, P.; Dannenberg, J. J.; Zakrzewski, V. G.; Dapprich, S.; Daniels, A. D.; Strain, M. C.; Farkas, O.; Malick, D. K.; Rabuck, A. D.; Raghavachari, K.; Foresman, J. B.; Ortiz, J. V.; Cui, Q.; Baboul, A. G.; Clifford, S.; Cioslowski, J.; Stefanov, B. B.; Liu, G.; Liashenko, A.; Piskorz, P.; Komaromi, I.; Martin, R. L.; Fox, D. J.; Keith, T.; Al-Laham, M. A.; Peng, C. Y.; Nanayakkara, A.; Challacombe, M.; Gill, P. M. W.; Johnson, B.; Chen, W.; Wong, M. W.; Gonzalez, C.; Pople, J. A. *Gaussian 03*, revision B.02; Gaussian, Inc.: Pittsburgh, PA, 2003.
(39) Meyers, F.; Marder, S. R.; Pierce, B. M.; Bredas, J. L. *J. Am. Chem. Soc.* **1994**, *116*, 10703.
(40) Nandi, P. K.; Mandal, K.; Kar, T. *Chem. Phys. Lett.* **2003**, *381*, 230.
(41) Parr, R. G.; Pearson, R. G. *J. Am. Chem. Soc*. **1983**, *105*, 7512.
(42) Oudar, J. L. *J. Chem. Phys*. **1977**, *67*, 446.
(43) Oudar, J. L.; Chemla, D. S. *J. Chem. Phys*. **1977**, *66*, 2664.